17-9-2021

An Innovative Energy Harvesting Shock Absorber System for Motorbikes

José Luis Olazagoitia

Jordi Viñolas

Alejandro González

Ibai Ulacia

Mikel Izquierdo

This is an Accepted Manuscript version of the following article, accepted for publication in:

An Innovative Energy Harvesting Shock Absorber System for Motorbikes

González A.[1], Olazagoitia J.L.[1*], Vinolas J. [1], Ulacia I. [2], Izquierdo M. [2]

Abstract—**This paper presents an innovative energy recovery shock absorber system for motorcycles. The shock absorber is named SP-EHSA (Synchronous Pulley - Energy Harvesting Shock Absorber). The SP-EHSA is the first system specifically designed to maximize the energy recovery of motorcycles without compromising their dynamic behavior. Throughout the article the theoretical design, computer modeling, optimization, design, and testing of the system is presented. The article results in a validated computer model of the SP-EHSA shock absorber. The validation is done by manufacturing and testing a physical prototype on a test bench. A study of the energy recovery potential for different road profiles at speeds between 20 km/h and 100 km/h was carried out, obtaining in a typical type B road at 60 km/h an estimated 19,68 W average power. Finally, the effect of energy management (i.e. battery's state of charge) on the dynamic behavior of the vehicle is analyzed.**

Index Terms—**EHSA, Energy Harvesting, Shock Absorber, Motorbike Suspension, Simulink/Simscape, Experimental Test**

I. INTRODUCTION

Traditional hydraulic suspensions have been commonly used in vehicles to reduce the accelerations suffered by the vehicle body (comfort) as well as to ensure the contact of the tires with the road (handling). The need to improve the energy efficiency of vehicles has led to the emergence of new innovative studies for energy recovery. Based on these studies, different technologies have been developed. These allow the recovery of part of the kinetic energy that was lost in the form of heat. Traditional suspensions damp the vehicle's vibrations by dissipating energy through pressure and heat friction losses when a fluid, commonly hydraulic oil, passes through calibrated holes. EHSA (Energy Harvesting Shock Absorbers) are characterized by their ability to convert some of the kinetic energy of the shock absorber into electrical energy.

EHSAs can be classified according to their principle of operation. The piezoelectric EHSA and the electromagnetic EHSA are differentiated. On the one hand, the piezoelectric EHSA uses a piezoelectric material for the generation of electrical energy. Their impossibility to generate a damping force like that of a traditional suspension, forces them to act as a complementary system to a main suspension system. This situation limits the energy recovery potential of this technology. In [1] the implementation of a multi-layer piezoelectric vibration EHSA for the increase of the total energy recovered is designed, modeled and analyzed. The generated power is very low (0.5 mW) and it is proposed as a power supply system for external sensors as in [2]. In [3], a dimensionless analysis method is detailed for the prediction of the output voltage and recovered power for an EHSA piezoelectric system. One of the only existing piezoelectric EHSA prototypes is presented in [4]. Finally, in [5] the performance of a multi-layer piezoelectric MEMS (MicroElectroMechanical Systems) device for power generation is evaluated and improved. Therefore, it is concluded that the EHSA piezoelectric technology is not the most suitable to recover a high amount of energy from the suspensions. This type of EHSAs must work in parallel to a traditional suspension due to its lack of capacity to generate forces. It is then relegated to the supply of external sensors or to systems that require little electrical power to operate.

On the other hand, the electromagnetic EHSAs have been the most studied by researchers in the last two decades. Within this technology, we can find linear electromagnetic EHSAs and rotary electromagnetic EHSAs. The linear electromagnetic damper transforms the kinetic energy of the vertical oscillations of the vehicle directly into electrical energy by means of electromagnetic induction. Its main difference with the rotary electromagnetic damper is that the latter needs a transmission system to transform the linear oscillating movement into a rotary one in the generator.

Different studies develop linear electromagnetic EHSA. In [6] a hybrid suspension system is developed using a linear DC (Direct Current) generator. The aim of the study is the reduction of energy consumption in active suspensions. In [7] a prototype of a linear electromagnetic EHSA is developed based on linear generators for the recovery of energy in the suspension of a vehicle. This system is heavy due to the coil and magnets in the suspension travel. In [8] the design and optimization of different linear electromagnetic transducers for energy recovery in large-scale vehicle suspensions is presented. With such optimization, they achieve performances of up to 3.8 times the system presented in [7]. This system can recover 2.8 W power at speeds of 0.11 m/s. It is estimated that the system will have a power of up to 33 W at speeds of 0.25 m/s and a damping coefficient of 1680-2142 Ns/m. Due to the high weight that characterizes the linear electromagnetic EHSA, studies like [9],

[1] A. González, J.L. Olazagoitia and J. Vinolas, Department of Industrial and Automotive Engineering (DIIA). Universidad Antonio de Nebrija. C/Pirineos 55, 28040 – Madrid, (Spain) (e-mail: jolazago@nebrija.es).

[2] I. Ulacia I. and M. Izquierdo, Structural Mechanics and Design, Dept. Mechanical and Industrial Production, Faculty of Engineering, Mondragon Unibertsitatea

[10] and [11] arise in which the relative speed between the magnetic field and the winding is optimized, increasing the efficiency and decreasing part of the weight. In these systems recovered power is around 16 W for speeds of 0.25 m/s and 64 W for speeds of 0.50 m/s. [12] and [13] presents an optimal design of an exterior permanent magnet tubular machine for energy harvesting from vehicles suspension systems with values of 210.2 and 103.7 W maximum recovered. Linear electro-magnetic EHSAs may seem the most suitable for recovering the energy dissipated in traditional shock absorbers, since they do not need any adaptation of the movement and reduce energy losses. However, this technology presents two main issues. On the one hand, the mass of the permanent magnets, the winding, and the ferromagnetic core cause the total weight of the suspension to be up to 3 times greater than that of a traditional suspension. This increase in the unsprung mass of the vehicle has a direct influence on its dynamic behavior [14]. In addition, since there is no multiplication phase, the optimal speeds for energy recovery are not obtained. This is because energy recovery depends on the relative speed within an electromagnetic system. The linear EHSA does not have a multiplication phase and the relative speed is limited to the speed of the suspension. For these reasons, the rotating electromagnetic EHSAs are preferred and most researchers focus on them rather than the linear ones.

Finally, the rotating electromagnetic EHSAs transform kinetic energy (vibration according to the vertical axis of the vehicle) into electrical energy by using a rotating electromagnetic generator. EHSAs based on mechanical transmission electromagnetic technology are one of the most developed systems in the scientific literature. Its compactness, high conversion efficiency and ease of construction make the development of prototypes simple. These systems are classified according to the method used for motion transmission. First, there are the EHSAs that use a ball screw system to perform the motion conversion. These are known as BS-EHSA (Ball Screw). [15] and [16] present methodologies for the development of these systems obtaining power values up to 35 W with damping coefficients up to 3000 Ns/m. In [17] a high efficiency shock absorber for vehicles is proposed which provides a damping coefficient of 10580 Ns/m and recoveries of up to 7 W. In [18], an active control method of damping and energy reclaiming from a BS-EHSA is proposed using independently-controlled slot winding transducers . In [19] and [20] the rectification of motion for BS-EHSA shock absorbers is suggested. In [21], a new-type of mechanical-motionrectifier-based energy harvesting shock absorber using a ball-screw mechanism and two one-way clutches is proposed to replace conventional oil dampers in vehicle suspensions. In [22], a BHSA system with independent generators is developed to optimize the damping force and energy recovery. Other publications deal with the Inerter phenomenon in these systems as [23] and [24]. Finally, publications like [25] deal with the influence of friction parameters on the dynamic behavior and the recoverability of the suspension. Secondly, there are the EHSAs that use a rack and pinion mechanism for movement conversion. These are known as RP-EHSA (Rack and Pinion). Studies such as [26] model and analyze an RP-EHSA system with emphasis on the backlash effect. Another study like [27] presents the modeling and testing of a prototype. An average power of 19W is obtained for a vehicle driven at 40 km/h. There are studies where systems with gyro rectification are developed, such as [28], [29] and [30]. Power outputs between 3.6 W and 15.4 W are obtained.

Thirdly, there are studies that develop shock absorbers based on hydraulics. In [31], [32] and [33], the design, modeling and performance study of H-EHSA (Hydraulic) shock absorbers are presented. In [34] and [35], systems for heavy vehicles are developed. These obtain powers from 41.72 W to 339.88 W for speeds from 30 km/h to 70 km/h. Rectified systems (which allow for one direction turns only) can also be found ([36], [37] and [38]) showing powers of up to 110 W . In [39], a Human-knowledge-integrated Particle Swarm Optimization (Hi-PSO) scheme to globally optimize the design of the Hydraulic-electromagnetic Energy-harvesting Shock Absorber (HESA) for road vehicles is proposed. At 20 mm/1.5 Hz conditions, efficiencies of 59.07% are obtained.

Finally, the Cable Drive EHSA (CD-EHSA) is presented in [40]. In the study, powers of 25 W per shock absorber are obtained for speeds between 20 and 30 km/h with a conversion efficiency of up to 60%.

There are studies that address the control of EHSA systems for energy recovery. In [41] and [42], a multi-objective H∞ active control design methodology for EHSA systems is proposed. In [43], a generalized control design approach is presented for EHSA systems applied to civil engineering applications.

This article studies the use of a new EHSA system instead of traditional oil shock absorbers in motorcycles for the recovery of mechanical energy. The motorcycle used in this investigation is a lightweight electrically powered vehicle. As reviewed in the state of the art there are two main systems for energy recovery, the piezoelectric EHSAs and the electromagnetic EHSAs. The first are discarded because of their low energy recovery capacity and zero damping capacity. On the other hand, within the electromagnetic dampers we find the linear and the rotational ones. The first ones have a great mass that affects negatively the vehicle dynamics and is not able to reach optimal speeds for energy recovery. The second ones (the rotational electromagnetic EHSA) have been the most studied. Within these systems, the BS-EHSA and CD-EHSA shock absorbers are the most promising according to the literature. Based on the study included in [25], where the recoverable energy in both technologies is compared, the CD-EHSA system manages to generate between 80% and 110% more power than the BS-EHSA system. In addition, the Inerter effect produced is lower compared to the other technologies presented. One of the problems of the CD-EHSA system is the sliding of the cable when the tension is not appropriate. It was observed that in the application the bearings could not withstand the stress required for the operation of the CD-EHSA system. To solve this problem and to be able to make a more compact system, it was decided to replace the cable system with a timing belt. This type of belt has teeth that guarantee the synchronism of the belt [44]. Therefore, in the present article a rotational electromagnetic EHSA system by means of a transmission system by pulleys and synchronous belt for motorcycles is developed.

Therefore, the systems existing so far are not valid for light motorcycles as they either do not produce enough energy (piezoelectric EHSA) or increase considerably the unsprung mass of the vehicle (linear EHSA). Within the rotational

electromagnetic EHSAs (the most suitable for motorcycle applications) the one with the least inerter effect is the CD-EHSA. Consequently, this paper presents the development of a synchronous pulley recovery shock absorber (an evolution of the CD-EHSA system). It will be used in a light electric motorcycle offering a compact system with high energy recovery capacity.

The remainder of the article is divided into several sections. Section II presents the methodology and development of differential equations and the computational model. Section III presents the prototype of the EHSA shock absorber. Section IV validates the computational model by introducing the effect of friction. In V the energy study of the shock absorber is carried out and in VI the effect of the energy management on the dynamic behavior of the shock absorber is analyzed. Finally, in VII the conclusions are presented.

II. METHODOLOGY AND MODEL

In this section, an EHSA rotational electromagnetic transmission system by synchronous pulleys and belts (SP-EHSA) is developed for an electric motorcycle. This damper system employs a synchronous belt that travels between two pulleys. This belt (5M) has teeth that allow a synchronous movement of the whole mechanism avoiding slippage and allowing the installation of position sensors for future suspension control. The alternative motion of the suspension caused by the movement of the vehicle is transformed into a rotational movement by the synchronous pulley and belt system. The movement is then corrected by 90° using bevel gears and finally amplified by means of a multiplier to obtain the most efficient speeds for power generation. This type of transmission has not been published in other publications. The SP-EHSA is intended to be an evolution of the CD-EHSA cable transmission system presented in [45]. The following methodology has been followed. First, differential equations are developed to model the electromechanical operation of the SP-EHSA shock absorber. Then, a computational model using MATLAB/Simscape is generated. Once the model is developed, it is validated against the differential equations of the system. Subsequently, a prototype of SP-EHSA is designed and manufactured. This prototype is intended to be installed on an electric motorcycle without having to make additional modifications to the chassis of the vehicle. Then, this prototype is tested on a bench, which allows to adjust and validate the computer model with respect to the physical system. Finally, an analysis of the energy recovery potential is carried out by simulating the shock absorber in a 4DOF (Degrees of Freedom) model of the motorcycle.

A. Analytical model

The differential equations and model of the SP-EHSA shock absorber are developed. The rotating elements present in the regenerative suspensions have a significant influence due to their rotational inertia [25]. In order to model the influence of inertias, an equivalent mass (m_{eq}) is introduced in parallel to the system's damping (c_{eq}). This equivalent mass is called Inerter [2-3]. In addition, the use of non-rigid elements such as the synchronous belt also generates an equivalent stiffness (k_{eq})

in parallel with the system's damping. This equivalent modelling of the suspension is introduced in [48]. Figure 1 represents the dynamic equivalence of an SP-EHSA shock absorber.
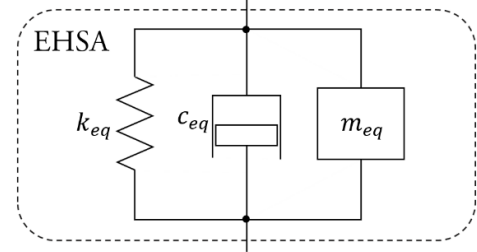

Figure. 1. Dynamic equivalence for an EHSA shock absorber

The modelling of the rotational electromagnetic generator is carried out by obtaining the different differential equations that characterize the generator and the connected load. In this way, it is possible to obtain the equivalent values of mass (m_e), damping ratio (c_e) and stiffness (k_e) of the electrical system. The modelling of the mechanical power entering the engine generator is carried out by means of Newton's law, where K_i is the torque constant, K_{gen} the voltage constant, U_{gen} the electrical potential, J_{gen} the rotational inertia and τ_r the resistant torque of the generator. The mechanical energy to the system is given by the torque coming from the τ_{mul} gearbox and the angular displacement of the shaft with respect to the θ_{mul} motor. R_i and L_i represent the internal resistance and inductance of the generator respectively and R_c and L_c represent the resistance and inductance of the connected load. Figure 2 shows the electrical diagram of the SP-EHSA shock absorber
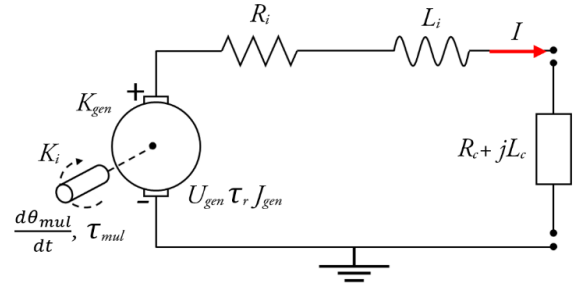

Figure. 2. Simplified electric circuit diagram of the SP-EHSA shock absorber.

Applying Newton's law, the equations for an ideal generator and Kirchhoff's law, equations (1), (2) and (3) are obtained which parameterize the values of mass, damping coefficient and equivalent stiffness of the electrical system respectively.

$$m_e = J_{gen} \tag{1}$$

$$c_e = \frac{K_i K_{gen}(R_i + R_c)}{(R_i + R_c)^2 + L_i^2 \omega^2} \tag{2}$$

$$k_e = \frac{K_i K_{gen} L_i \omega^2}{(R_i + R_c)^2 + L_i^2 \omega^2} \tag{3}$$

Next, the equations that characterize the mechanical system of the SP-EHSA shock absorber are developed. These equations together with those of the electrical system form the equivalent electromechanical system of the shock absorber. Figure 3

represents the diagram and constituting elements of the suspension mechanism. The linear reciprocating movement entering the suspension with a force F_1 and an x displacement is converted to a rotational movement with torque τ_{pp} and angular displacement θ_{pp} by means of the synchronous pulley and belt system. The rotational movement is then brought to a perpendicular axis by two bevel gears with a ratio of 1:1. The torque on the new shaft has a value of τ_{ec} and an angular displacement of θ_{ec}. Finally, the revolutions entering the generator are increased by implementing a gearbox. This converts the outgoing torque and angular displacement of the bevel gears into τ_{mul} and θ_{mul}, which is the input to the generator. The synchronous belt of the pulley system is modelled with a stiffness k_c. k_p and c_c correspond to the stiffness and damping coefficient of the tensioner respectively. T_1, T_2 and T_3 represent the tensions suffered by the belt. The idler pulley will rotate at an angular speed of $\dot{\theta}_l$ and has a radius r_{pl}. Likewise, the generating pulley has a radius r_{pp}.
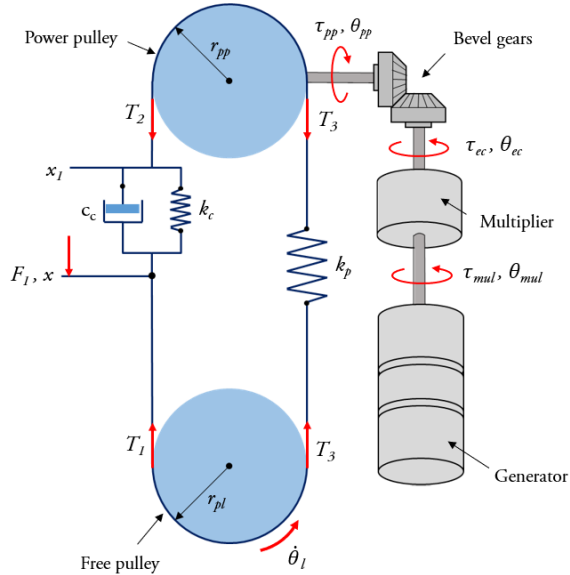

Figure. 3. Diagram of the equivalent mechanical system of the SP-EHSA shock absorber.

Applying the equations that govern the mechanical movement of the SP-EHSA shock absorber in the different stages together with equations (1), (2) and (3), equations (4), (5) and (6) are obtained that make up the equivalent electromechanical system of the shock absorber. Where $J_{pl}, J_{pp}, J_{ec}, J_{mul}$ and J_{gen} are the inertias of the freewheel, power pulley, bevel gears, multiplier and generator respectively. η_{pp}, η_{ec} and η_{mul} are the performances of the power pulley, bevel gears and multiplier respectively. Finally, k_{ec} and k_{mul} are the multiplication factors of the bevel gears and the planetary gearbox.

$$m_{eq} = \frac{k_{ec}^2 k_{mul}^2 (J_{gen} + J_{mul})}{r_{pp}^2 \eta_{pp} \eta_{ec} \eta_{mul}} + \frac{k_{ec}^2 J_{ec}}{r_{pp}^2 \eta_{pp} \eta_{ec}} + \frac{J_{pp}}{r_{pp}^2 \eta_{pp}} \quad (4)$$

$$c_{eq} = \frac{k_{ec}^2 k_{mul}^2 K_i K_{gen} (R_i + R_c)}{r_{pp}^2 \eta_{pp} \eta_{ec} \eta_{mul} ((R_i + R_c)^2 + L_i^2 \omega^2)} \quad (5)$$

$$k_{eq} = \frac{k_{ec}^2 k_{mul}^2 K_i K_{gen} L_i \omega^2}{r_{pp}^2 \eta_{pp} \eta_{ec} \eta_{mul} ((R_i + R_c)^2 + L_i^2 \omega^2)} \quad (6)$$

B. Computational model

Once the differential equations of the SP-EHSA system are obtained, the computer model is developed. For this purpose, the MATLAB/Simulink/Simscape software is used. The software has pre-determined subsystems that represent the different mechanical and electrical elements that make up the model. The system of synchronous pulleys, the gear train, the gearbox and the electrical circuit are represented in Figure 4. The block that represents the pulleys has its inertia value integrated. The same applies to the generator block, where the resistance values and internal impedances are also included. The inertia of the gear system and the gearbox is represented in the form of Inerter. A purely resistive load is connected to the generator to simplify the calculation of power and damping coefficient. Figure 4 shows the computational model of the SP-EHSA damper model in a Simulink/ Simscape environment.
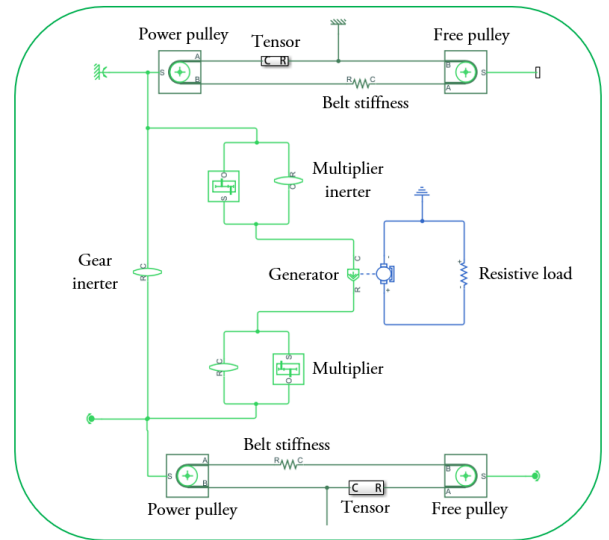

Figure. 4. Computer model of the SP-EHSA shock absorber made in the Simscape software.
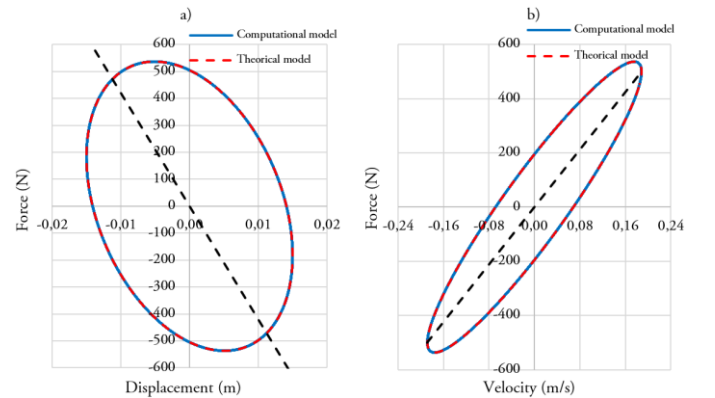

Figure. 5. Theoretical and computational model of an SP-EHSA for a sinusoidal incoming signal. a) Displacement with respect to force. b) Speed with respect to force.

The computational model is compared with the differential equations to validate its use. From this moment on, the computer model is used for the simulations of the paper. For this purpose, a simulation is carried out for a fixed connected resistance of 5 Ω and a sinusoidal displacement signal. The result of both models is shown in Figure 5. As can be seen, the dynamic behavior is equivalent and has the same damping coefficient.

III.   PROTOTYPE DEVELOPMENT

The design of the SP-EHSA shock absorber is performed considering the geometrical and functional restrictions of the motorbike's rear shock absorber. Due to space restrictions a very compact design is required. In addition, it must satisfy the requirements for optimum performance in energy recovery. The radius of the generating pulley combined with the conversion factor of the gearbox are the most influential mechanical parameters in the behavior of the regenerative shock absorber. According to the literature, a linear-rotational displacement conversion of 4 to 6 mm/rev is recommended [49]. Considering this recommendation and after a sensitivity analysis of the parameters selected together with the commercial offer, a $r_{pp} =$ 20 mm and a $k_{mul} = 13.5$ are considered. The maximum displacement of the suspension is limited to 40 mm due to geometrical restrictions. The conversion mechanism from linear to rotational movement is integrated in the main cylinder of the shock absorber. The spring (which is not shown in the sketch) that gives the rigidity to the suspension surrounds this cylinder and is delimited by two adjustable nuts that allow varying the preload force.

The conversion of linear movement into rotational movement is carried out by a system of synchronous pulleys and belts (figure 6 "1"). The vertical oscillating movement of the suspended mass of the motorbike is anchored to the upper joint of the shock absorber by means of a ball joint that allows the oscillating movement of the suspension arm (figure 6 "2"). The linear movement is transmitted to a piston that is attached to the strap's crimp block (figure 6 "3"). This block is connected to a linear ball bearing guide system (figure 6 "4"). The linear guide is attached to the suspension cylinder. The cylinder is connected to the lower suspension bracket with another ball joint (figure 6 "5"). The clamping block is connected to the synchronous belt by two clamping elements with the belt profile. The belt is located between two synchronous pulleys. The first rotates freely, while the second is responsible for transmitting the power.

The synchronous pulleys are fixed to two shafts that rotate on a system of bearings. The power shaft transmits the energy to a system of 2 bevel gears (figure 6 "6") that correct the rotation axis by 90º. Both gears are identical, maintaining a gear ratio of 1:1. The power output from the gear system is transmitted to a planetary gearbox (figure 6 "7") with a ratio of 1:13.5. The output of the gearbox is fed into the DC generator (figure 6 "8"). The prototype is made of duralumin 7075. This alloy has high mechanical performance and low density, which allows for a substantial reduction in the total weight of the

suspension with only 1.45 kg including the electric generator. The manufactured prototype is shown in Figure 7.
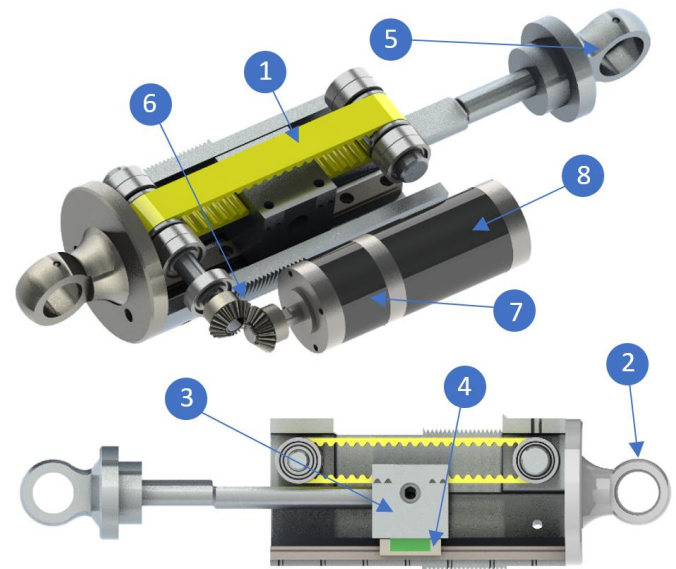

Figure. 6. CAD design of the EHSA prototype with its electromechanical components

According to the datasheets of the manufacturers of the different elements, the following mechanical efficiencies are obtained. The 5M timing belt, the 2-stage planetary gearbox and the bevel gears have an efficiency of 98%, 87% and 95% respectively.
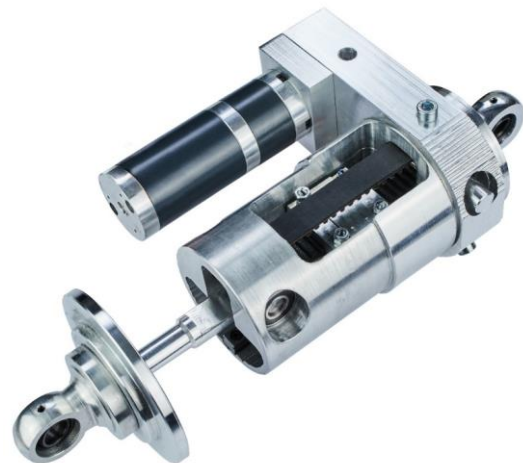

Figure. 7. Prototype of the SP-EHSA shock absorber made of 7075 aluminum with the gearbox and the electric generator

Once the prototype has been manufactured, a series of experimental tests are carried out in the DMELab laboratory of Mondragon Unibertsitatea. For this purpose, a specially designed test bench is used for testing dampers such as vehicle's corners or complete suspensions [50]. The prototype is subjected to a series of sinusoidal signals with an amplitude of 2.5, 5, 7.5 and 10 mm and a frequency of 0.5, 1, 2, 3 and 4 Hz. Likewise, different values of a purely resistive load are installed on the generator of 2, 6, 10, 15, 47 and 94 Ω. In the tests, the displacement of the piston that performs the

movement, the force caused by the SP-EHSA and the voltage generated between the terminals of the resistive load R_c are recorded. Figure 8 shows the test bench used in the different experimental tests.
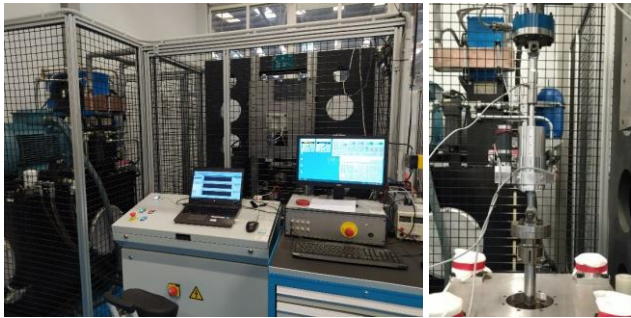

Figure. 8. SP-EHSA prototype being tested on a specialized Mondragon Unibertsitatea test bench.

Figure 9.a shows the force performed by the SP-EHSA in relation to the speed for different load values R_c and a sinusoidal excitation signal with an amplitude of 10mm and a frequency of 0.5 Hz. There is a clear correlation between the load on the electrical circuit and the force exerted by the system. When the resistance is zero (short circuit case) the force reaches the maximum values. On the other hand, when the terminals of the DC generator are open, the minimum force that can be exerted by the damper appear. Therefore, by varying the resistance between both ends we can obtain different slopes and therefore values of the system's damping coefficient. Some oscillations are observed at the ends of the force-velocity curve due to the EHSA mechanical elements. On the other hand, figure 9.b shows the force exerted by the SP-EHSA shock absorber with respect to the displacement for the same situation as in the previous case. The same correlation can be observed as in the case of speed, with greater forces appearing as the resistance connected to the circuit decreases. We can appreciate certain irregularities in the oval that are caused by internal clearance and friction of some of the mechanical elements of the shock absorber.

IV. MODEL VALIDATION

The validation of the SP-EHSA's computational model is carried out through a series of dynamic and quasi-static bench tests. The computational model presented in the previous section considers an ideal system without energy losses between each of the mechanical elements. In other words, the model does not consider the friction between the different moving elements that make up the system. The existence of friction in the mechanisms of the prototype has an influence on the experimental results obtained. For this reason, the model is complemented by introducing a simplified effect of these frictions. The most representative friction parameters in the dynamic behavior of the shock absorber are given in the linear guide, the bearings, the gearbox and the generator. For simplification purposes, a single rotational friction is considered where the Coulomb friction parameters T_{cu} and the

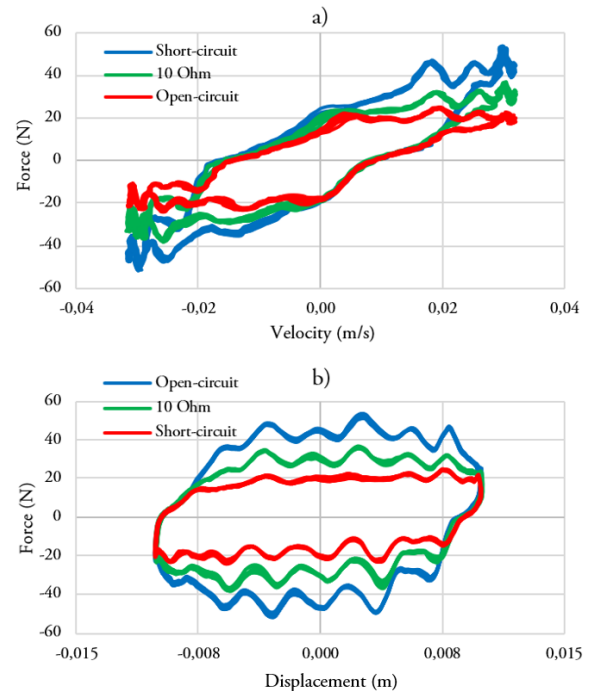viscous coefficient f_{vi} are considered.

Figure. 9. Force results of the SP-EHSA prototype for different R_c loads and a 10mm 0.5Hz sine wave amplitude displacement signal. a) Force-velocity. b) Force-displacement.

Firstly, static friction is estimated using data obtained from quasi-static experimental tests. A triangular displacement signal (constant speed and force) with an amplitude of 10mm at a frequency of 0.03 Hz is used. A purely resistive load of value $10\ \Omega$ is installed on the generator. During the tests, the time, displacement, force and voltage generated are acquired for comparison with the results of the computer model. In this situation (speed close to 0 m/s), the generator and the dynamic friction have no effect on the force exerted by the shock absorber. Figure 10.a shows the piston displacement during the quasi-static test. A SQP (Sequential Quadratic Programming) local optimization algorithm is applied to reduce the error of the simulated force with respect to the experimental one. A final value of T_{cu} of 0.0327 Nm is obtained. Figure 10.b represents the simulated force with respect to the experimental one for a computational model without friction while figure 10.c includes the Coulomb friction in the computational model.

Once the Coulomb friction has been estimated, the viscous coefficient is estimated by means of dynamic tests. Different dynamic tests are carried out where a triangular signal of amplitudes 5 mm and 10 mm and frequencies of 0.5, 2 and 4 Hz are introduced. No representative influence of the viscous coefficient is observed in the resulting error of the simulated force with respect to the experimental one. That is why the parameter of the model is eliminated.

Once the effect of friction is included in the model, the results of the computational model are represented with respect to the SP-EHSA prototype. Figure 11 represents a comparison between the experimental tests and the simulations for a triangular profile displacement. Figure 11.a shows the force and voltage values for a test with 20mm travel and 0.5 Hz. A

correlation is observed in both chaos with an NRMSD (Normalized Root-Mean-Square Deviation) error of 4.52% and 5.12% for the force and voltage, respectively. The effect of the backlash (caused by the different mechanical elements of the system) on the generation of the voltage can be seen. Figure 11.b shows the force and voltage for a 10 mm and 2 Hz displacement signal. A lower correlation is observed in the force where the NRMSD increases up to 8.27%. The error in voltage is 6.12%. Finally, Figure 11.c shows the force and speed for a signal of 10mm amplitude and 4Hz. In this case the error increases to 14.5%. The NRMSD of the voltage is maintained at 6.24%.
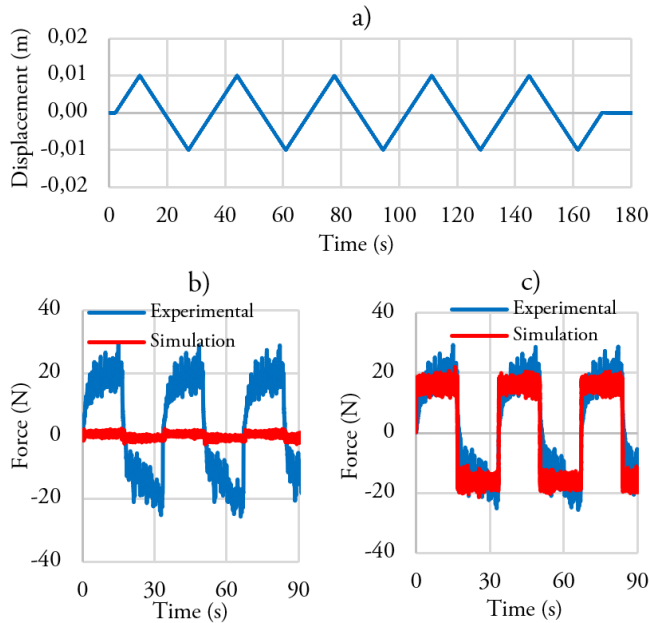

Figura. 10. Coulomb friction test results. (a) suspension displacement. (b) Simulated versus experimental force without friction (c) Simulated versus experimental force with friction.
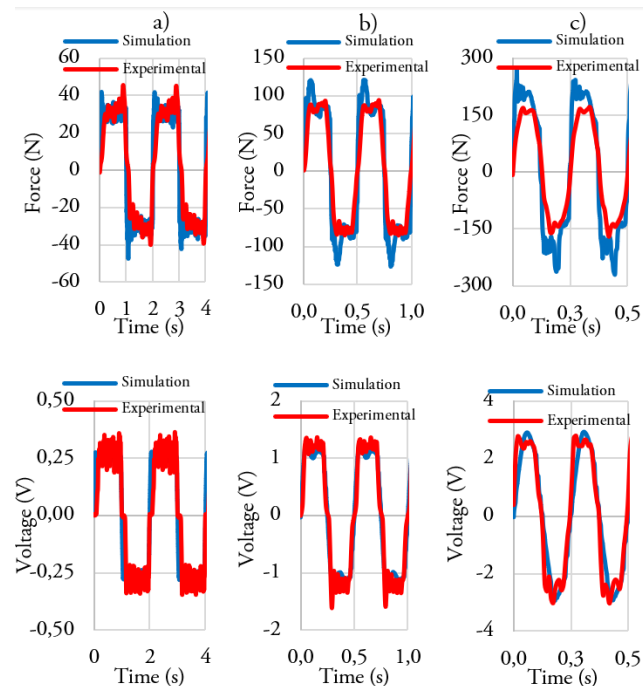

Figure. 11. Comparison of the experimental prototype with the model for a triangular displacement of 10mm amplitude. (a) Frequency of 0.5Hz. (b) Frequency of 2Hz. (c) Frequency of 4Hz.

Figure 12 shows the voltage generated in an experimental test and a simulation with a sinusoidal displacement with a small amplitude. The substantial effect of the backlash on power generation can be seen. The backlash also affects the damping capacity of the SP-EHSA. The backlash effect is not introduced in the model. This effect is produced by the variation of the rotation direction in compression and extension. Rectification of the system's direction of rotation would eliminate this effect.
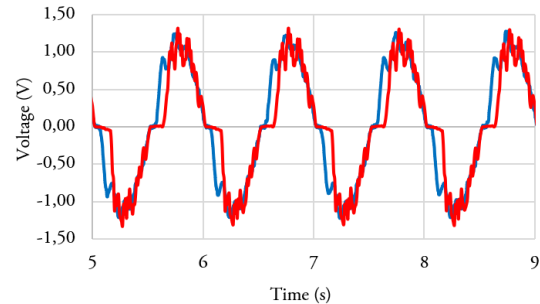

Figure. 12. Backlash effect on the experimental voltage with respect to that simulated by the SP-EHSA when it is subjected to a low-amplitude sinusoidal displacement.
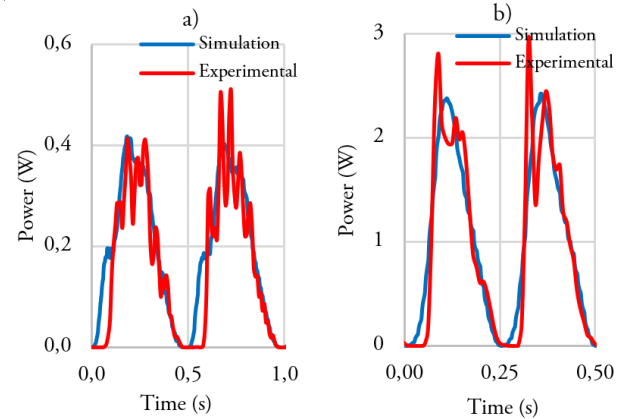

Figure. 13. Experimental and simulated power obtained by the SP-EHSA prototype (a) For a sinusoidal displacement of 5mm and 1Hz. (b) For a sinusoidal displacement of 10mm and 2Hz.

Due to the characteristics of the generator (internal resistance and constant generator voltage), the power obtained in the tests is lower than expected, reaching up to 2.5W. The figure 13 shows the power obtained for two tests and simulations with a sinusoidal displacement signal. In the figure 13.a the power obtained is 0.4W for a signal of displacement of amplitude 5mm and 1Hz, whereas in the figure 13.b the power obtained is up to 2.5W for a sinusoidal displacement of amplitude 10mm and 2Hz.

V. ENERGY STUDY

After validating the computer model of the SP-EHSA system, a study of the energy that can be recovered under different driving conditions is carried out. A series of simulations are performed where a flat 4 DOF model of a motorbike is used. The rear shock absorber is replaced by the

SP-EHSA. The generator is replaced by a suitable one to achieve the necessary damping coefficient for the motorbike (generator constant 0.098 V/(rad/s) and internal resistance 0.108 Ω). A compression resistor R_c of 6.80Ω and an extension resistor R_c of 3.01Ω are connected. The new generator has dimensions compatible with the prototype and motorcycle presented in this paper. The higher performance of the generator in the same dimensions results in an increase in the cost of the SP-EHSA.

The energy recovery during driving on a road without specific obstacles gives an idea of the power that can be recovered during driving on high-speed roads such as motorways and highways. To carry out this study, it is necessary to classify the different types of roadway into profiles according to their roughness. The longitudinal profiles represent the degree of roughness and the texture of a road. Their classification is based on ISO 8606. This standard proposes a differentiation of roughness using the Power Spectral Density (PSD). For paved roads, a classification of road classes from A to D is carried out.

A series of simulations are carried out to obtain the energy recovered in road profiles and speed values of 20 km/h, 40 km/h, 60 km/h, 80 km/h, 100 km/h and 120 km/h. Figure 14 shows the results of a simulation for a speed of 70km/h and a type B road. Figure 14.a shows the displacement of the front and rear tires of the motorbike. Figure 14.b represents the displacement of the rear suspension with respect to time. Finally, figure 14.c shows the instantaneous power produced by the shock absorber generator.
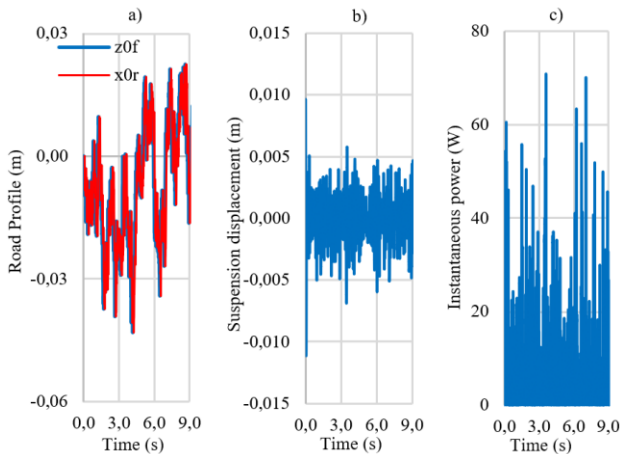

Figure. 14. Simulation results for a type B road profile. (a) road displacement, (b) suspension displacement and (c) instantaneous power.

The power results of the simulations are shown in Table I. The generated power values are presented in RMS (Root Mean Square) power. As the speed increases, the energy recovered is higher. Likewise, the greater the roughness of the road, the greater the power generated. The type of road has a greater effect than the speed of traffic on the amount of power generated.

TABLE I
GENERATED POWER DEPENDING ON THE ROAD PROFILE

Profile	20 km/h	40 km/h	60 km/h	80 km/h	100 km/h
A	1.23W	2.49W	3.79W	5.17W	6.42W
B	4.52W	9.84W	19.68W	35.36W	78.58W
C	16.78W	39.46W	78.72W	-	-
D	79.22W	156.52W	-	-	-
E	306.45W	-	-	-	-

The amount of energy that can be recovered by the shock absorber in a point bump at different speeds is then analyzed. For the study, the most common shoulder profile is selected for Spanish roads that follow the order FOM/3053/2008, which dictates the technical instruction for the installation of speed reducers and warning cross bands on roads. The obstacle has a circular profile of 300 mm width and 75 mm height. Simulations are performed for different speeds on the bump. These speeds are 10 km/h, 15 km/h and 20 km/h. Higher speeds are not suitable for crossing this type of overhang. Figure 15 shows the results of the simulations carried out. Figure 15.a shows the displacement of the rear shock absorber when crossing the bump. Figure 15.b shows the voltage produced by the generator. Finally, figure 15.c shows the instantaneous power generated.
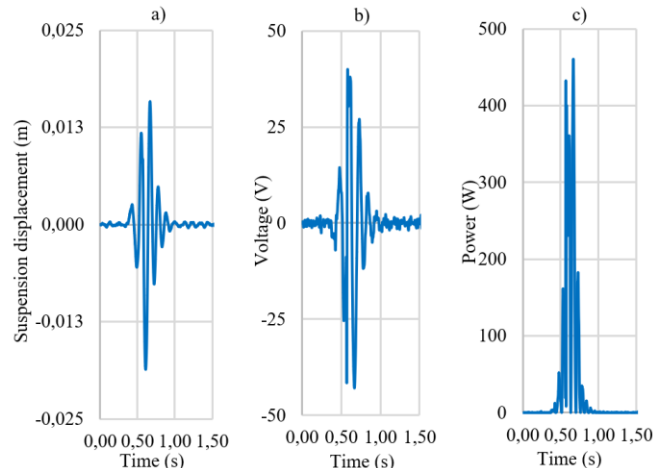

Figure. 15. Simulation results when passing through different relief profiles at constant speed. a) displacement, b) voltage generated and (c) power generated.

The average total power generated in the gearbox is obtained by calculating the area under the instantaneous power curve by means of numerical integration and dividing by the time (1 s in this case). The total power results generated are presented in Table II.

TABLE II
GENERATED AVERAGE POWER IN A SPEED REDUCER

Velocity	10 km/h	15 km/h	20 km/h
Average Power	14.67W/	31.39W/	47.38W/

The amount of energy generated during driving on a road with a good profile (A, B, and C) or driving through point bumps is not enough to supply the vehicle's main traction battery, but it does allow the supply of secondary systems.

Finally, the efficiency of the SP-EHSA system is obtained from the simulations performed previously. The difference between the power input to the snubber and the power recovered in the form of electrical energy is studied. Energy

management has not been included in the study. An average efficiency of 61.08% is obtained. Figure 16 shows an example of the recovered power for a sinusoidal type of motion.
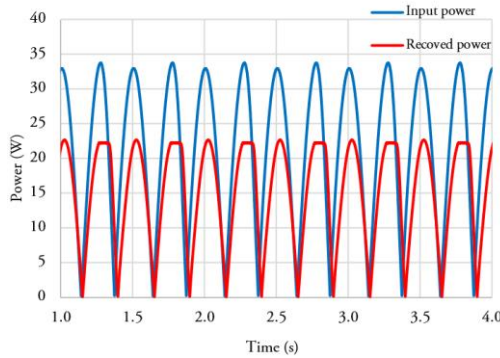

Figure. 16. Incoming power to the SP-EHSA system versus recovered electrical energy.

A comfort study of the SP-EHSA system for different electrical parameters and road conditions will be carried out in future works. Figure 17 shows a comparison between the acceleration of the suspended mass with the traditional oil suspension and the proposed EHSA system. The oil damper data were collected in experimental tests while the EHSA acceleration has been obtained by simulation for the passage of the motorcycle over a point obstacle. The similarity of both signals can be observed.
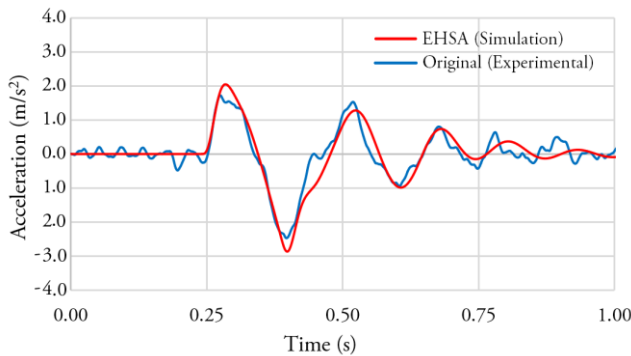

Figure. 17. Motorcycle sprung mass acceleration for the oil shock absorber and the EHSA system

VI. EFFECT OF ENERGY MANAGEMENT ON DYNAMIC BEHAVIOR

The influence of the energy management process on the dynamic behavior of EHSAs is presented below. In order to observe this phenomenon, a series of simulations were carried out. A simple electrical circuit is implemented using MATLAB/Simulink. The electrical schematic is represented in Figure 18 where the generator represents the model of the SP-EHSA system modeled in Simscape. Since the mechanical system of the SP-EHSA system does not have motion rectification, i.e. the direction of rotation on the generator shaft is opposite in extension and compression, a voltage adaptation must be made to ensure proper battery operation. A rectifier bridge is used for this purpose. A capacitor is then inserted to stabilize the input voltage to the last element, the battery. The capacitor filters input voltage peaks to prevent battery damage.
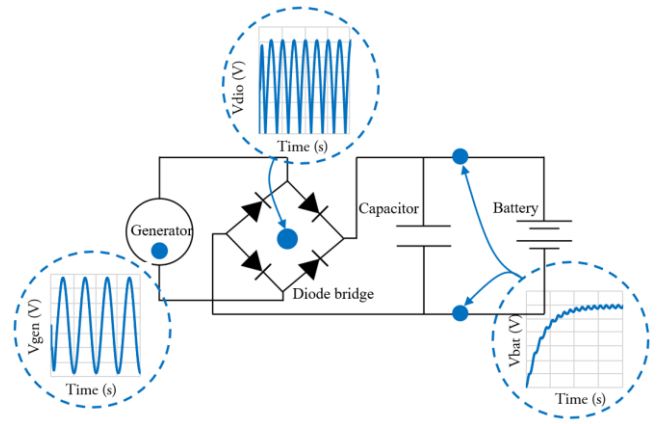

Figure. 18. Simplified electrical circuit for energy management in the SP-EHSA.

In the battery charging procedure, an effect of the stored voltage on the dynamic behavior of the EHSA shock absorber is observed. Figure 19 shows the variation of the damping curves according to the state of charge of the battery. A sinusoidal displacement signal with an amplitude of 0.04 m and a frequency of 1 Hz was used for the simulation. Figure 19.a shows the charging voltage of the battery as a function of time. In points 1, 2 and 3 of the Figure 18 the force-displacement and force-velocity curves of the shock absorber are analyzed. Figure 19.b shows the force-displacement diagram for the different battery states of charge.
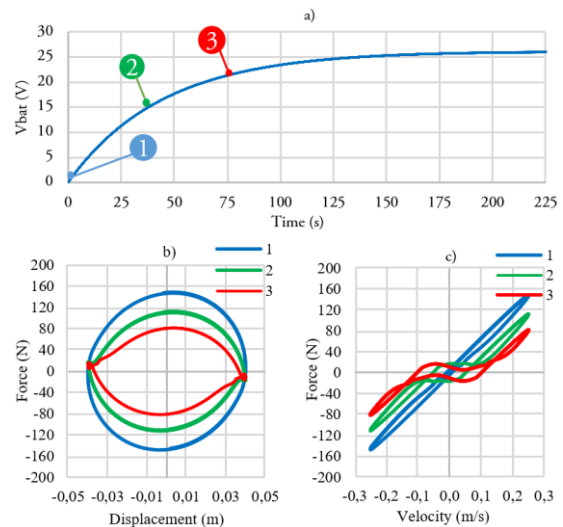
Figure. 19. Effect of the battery charge on the dynamic behavior of the SP-EHSA system (a) Battery voltage with respect to time. (b) Force-displacement curve for different battery states of charge (c) Force-velocity curve for different battery states of charge.

It can be seen how the average force exerted by the shock absorber decreases notably as the charging voltage increases. In addition, at the points where the travel is greater, there is a loss of the hysteresis phenomenon. On the other hand, Figure 19.c shows the force-velocity diagram for the different states of charge of the battery. As the stored voltage increases in the battery, a flattening of the curve is produced for low speeds. This represents the inability to generate damping force at low speeds, or in other words, when the voltage generated is lower

than the battery voltage [51]. The slope in the active zone of the shock absorber remains constant as the load connected to the system does not vary. Obviously, the fact that damping characteristics vary with the battery charge is a non-desirable effect. It is out of the scope of this paper to describe in detail the solutions that could be implemented to solve that problem, but it is important to point out that they are feasible but require some design process in order to optimize the energy management system itself.

VII. CONCLUSION

In this article the study, design, manufacture and experimentation of a prototype of the SP-EHSA shock absorber for motorcycles was presented. Firstly, a theoretical model based on the equations of the electromechanical components of the shock absorber was developed. With these equations the equivalent dynamic model of the shock absorber was obtained. Next, a computer model was developed in the Matlab/Simulink/Simscape software and validated against the theoretical model. The force-displacement and force-velocity curves were found to be equivalent. Based on the geometric and dynamic restrictions of the motorcycle, a prototype of the SP-EHSA was designed and manufactured. Several experimental tests were carried out to validate the computational model through the addition of friction parameters. The influence of Coulomb friction was observed. Once the model was validated, the energy recovery potential for different circulation situations was studied. The energy generation in the passage of a motorcycle through different road profiles was analyzed. It was observed that at higher traffic speeds and worse road conditions the energy recovery capacity is higher. Likewise, energy generation by a speed reducer obstacle was analyzed. Finally, an electrical system for storing the recovered energy was proposed. At this point, the influence of the battery voltage on the system's buffering capacity was observed and it was pointed out that this is an area where work is required to improve the energy management system

ACKNOWLEDGMENT

REFERENCES

[1]   W. Hendrowati, H. L. Guntur, and I. N. Sutantra, "Design, Modeling and Analysis of Implementing a Multilayer Piezoelectric Vibration Energy Harvesting Mechanism in the Vehicle Suspension," *Engineering*, vol. 04, no. 11, pp. 728–738, 2012, doi: 10.4236/eng.2012.411094.

[2]   B. Lafarge, C. Delebarre, S. Grondel, O. Curea, and A. Hacala, "Analysis and optimization of a piezoelectric harvester on a car damper," *Phys. Procedia*, vol. 70, pp. 970–973, 2015, doi: 10.1016/j.phpro.2015.08.202.

[3]   H. Xiao, X. Wang, and S. John, "A dimensionless analysis of a 2DOF piezoelectric vibration energy harvester," *Mech. Syst. Signal Process.*, vol. 58, pp. 355–375, 2015, doi: 10.1016/j.ymssp.2014.12.008.

[4]   H. X. Zou, W. M. Zhang, K. X. Wei, W. B. Li, Z. K. Peng, and G. Meng, "Design and Analysis of a Piezoelectric Vibration Energy Harvester Using Rolling Mechanism," *J. Vib. Acoust. Trans. ASME*, vol. 138, no. 5, 2016, doi: 10.1115/1.4033493.

[5]   C. Borzea and D. Comeagă, "Analysis and optimization of a piezoelectric energy harvester," *E3S Web Conf.*, vol. 112, 2019, doi: 10.1051/e3sconf/201911204001.

[6]   Y. Suda and T. Shiiba, "A new hybrid suspension system with active control and energy regeneration," *Veh. Syst. Dyn.*, vol. 25, no. SUPPL., pp. 641–654, 1996, doi: 10.1080/00423119608969226.

[7]   B. Scully, L. Zuo, J. Shestani, and Y. Zhou, "Design and characterization of an electromagnetic energy harvester for vehicle suspensions," *ASME Int. Mech. Eng. Congr. Expo. Proc.*, vol. 10, no. PART B, pp. 1007–1016, 2010, doi: 10.1115/IMECE2009-12091.

[8]   X. Tang, T. Lin, and L. Zuo, "Design and optimization of a tubular linear electromagnetic vibration energy harvester," *IEEE/ASME Trans. Mechatronics*, vol. 19, no. 2, pp. 615–622, 2014, doi: 10.1109/TMECH.2013.2249666.

[9]   N. V. Satpute, S. Singh, and S. M. Sawant, "Energy harvesting shock absorber with electromagnetic and fluid damping," *Adv. Mech. Eng.*, vol. 2014, 2014, doi: 10.1155/2014/693592.

[10]   D. Karnopp, "Permanent Magnet Linear Motors Used as Variable Mechanical Dampers for Vehicle Suspensions," *Veh. Syst. Dyn.*, vol. 18, no. 4, pp. 187–200, 1989, doi: 10.1080/00423118908968918.

[11]   S. Singh and N. V. Satpute, "Design and analysis of energy-harvesting shock absorber with electromagnetic and fluid damping," *J. Mech. Sci. Technol.*, vol. 29, no. 4, pp. 1591–1605, 2015, doi: 10.1007/s12206-015-0331-7.

[12]   M.-T. Duong and Y.-D. Chun, "Optimal Design of a Novel Exterior Permanent Magnet Tubular Machine for Energy Harvesting From Vehicle Suspension System," *IEEE Trans. Energy Convers.*, vol. 35, no. 4, pp. 1772–1780, Dec. 2020, doi: 10.1109/TEC.2020.2993211.

[13]   M.-T. Duong, Y.-D. Chun, P.-W. Han, B.-G. Park, D.-J. Bang, and J.-K. Lee, "Optimal Design of a Novel Single-Phase 8-Slot 8-Pole Tubular Electromagnetic Shock Absorber to Harvest Energy," *IEEE Trans. Ind. Electron.*, vol. 67, no. 2, pp. 1180–1190, Feb. 2020, doi: 10.1109/TIE.2019.2898591.

[14]   W. Wang, X. Chen, and J. Wang, "Unsprung Mass Effects on Electric Vehicle Dynamics based on Coordinated Control Scheme," in *2019 American Control Conference (ACC)*, 2019, pp. 971–976, doi: 10.23919/ACC.2019.8814981.

[15]   B. Huang, C. Y. Hsieh, F. Golnaraghi, and M. Moallem, "Development and optimization of an energy-regenerative suspension system under stochastic road excitation," *J. Sound Vib.*, vol. 357, pp. 16–34, 2015, doi: 10.1016/j.jsv.2015.07.004.

[16]   N. Amati, A. Festini, and A. Tonoli, "Design of electromagnetic shock absorbers for automotive suspensions," *Veh. Syst. Dyn.*, vol. 49, no. 12, pp. 1913–1928, 2011, doi: 10.1080/00423114.2011.554560.

[17]   Y. Wang, Z., Zhang, T., Zhang, Z., Yuan, Y., & Liu, "Wang, Z., Zhang, T., Zhang, Z., Yuan, Y., & Liu, Y. (2019). A high-efficiency regenerative shock absorber considering twin ball screws transmissions for application in range-extended electric vehicles."

[18]   L. Xie, J. Li, S. Cai, and X. Li, "Electromagnetic Energy-Harvesting Damper With Multiple Independently Controlled Transducers: On-Demand Damping and Optimal Energy Regeneration," *IEEE/ASME Trans. Mechatronics*, vol. 22, no. 6, pp. 2705–2713, Dec. 2017, doi: 10.1109/TMECH.2017.2758783.

[19]   Q. N. Wang, S. S. Liu, W. H. Wang, and H. Wei, "Structure design and parameter matching of ball-screw regenerative damper," *Jilin Daxue Xuebao (Gongxueban)/Journal Jilin Univ. (Engineering Technol. Ed.)*, vol. 42, no. 5, pp. 1100–1106, 2012.

[20]   Y. Liu, L. Xu, and L. Zuo, "Design, Modeling, Lab, and Field Tests of a Mechanical-Motion-Rectifier-Based Energy Harvester Using a Ball-Screw Mechanism," *IEEE/ASME Trans. Mechatronics*, vol. 22, no. 5, pp. 1933–1943, 2017, doi: 10.1109/TMECH.2017.2700485.

[21]   Y. Liu, L. Xu, and L. Zuo, "Design, Modeling, Lab, and Field Tests of a Mechanical-Motion-Rectifier-Based Energy Harvester Using a Ball-Screw Mechanism," *IEEE/ASME Trans. Mechatronics*, vol. 22, no. 5, pp. 1933–1943, Oct. 2017, doi: 10.1109/TMECH.2017.2700485.

[22]   L. Xie, S. Cai, G. Huang, L. Huang, J. Li, and X. Li, "On Energy

Harvesting From a Vehicle Damper," *IEEE/ASME Trans. Mechatronics*, vol. 25, no. 1, pp. 108–117, Feb. 2020, doi: 10.1109/TMECH.2019.2950952.

[23] W. Bao, "Main Parameters Analysis of Ball Screw Shock Absorber on Suspension System Performance," *SAE Tech. Pap.*, vol. 2015-April, no. April, 2015, doi: 10.4271/2015-01-1504.

[24] J. Yin, X. Chen, J. Li, and L. Wu, "Investigation of equivalent unsprung mass and nonlinear features of electromagnetic actuated active suspension," *Shock Vib.*, vol. 2015, 2015, doi: 10.1155/2015/624712.

[25] L. Bowen, J. Vinolas, and J. L. Olazagoitia, "Design and Potential Power Recovery of Two Types of Energy Harvesting Shock Absorbers," *Energies*, vol. 12, no. 24, p. 4710, Dec. 2019, doi: 10.3390/en12244710.

[26] Z. Li, Z. Brindak, and L. Zuo, "Modeling of an electromagnetic vibration energy harvester with motion magnification," *ASME 2011 Int. Mech. Eng. Congr. Expo. IMECE 2011*, vol. 7, no. PARTS A AND B, pp. 285–293, 2011, doi: 10.1115/imece2011-65613.

[27] Z. Li, L. Zuo, G. Luhrs, L. Lin, and Y. X. Qin, "Electromagnetic energy-harvesting shock absorbers: Design, modeling, and road tests," *IEEE Trans. Veh. Technol.*, vol. 62, no. 3, pp. 1065–1074, 2013, doi: 10.1109/TVT.2012.2229308.

[28] Z. Li, L. Zuo, J. Kuang, and G. Luhrs, "Mechanical motion rectifier based energy-harvesting shock absorber," *Proc. ASME Des. Eng. Tech. Conf.*, vol. 6, pp. 595–604, 2012, doi: 10.1115/DETC2012-71386.

[29] Z. Zhang *et al.*, "A high-efficiency energy regenerative shock absorber using supercapacitors for renewable energy applications in range extended electric vehicle," *Appl. Energy*, vol. 178, pp. 177–188, 2016, doi: 10.1016/j.apenergy.2016.06.054.

[30] M. Liu *et al.*, "Design, simulation and experiment of a novel high efficiency energy harvesting paver," *Appl. Energy*, vol. 212, pp. 966–975, 2018, doi: 10.1016/j.apenergy.2017.12.123.

[31] Y. Zhang, X. Zhang, M. Zhan, K. Guo, F. Zhao, and Z. Liu, "Study on a novel hydraulic pumping regenerative suspension for vehicles," *J. Franklin Inst.*, vol. 352, no. 2, pp. 485–499, 2015, doi: 10.1016/j.jfranklin.2014.06.005.

[32] S. J. Anderson ZM, Giovanardi M, Tucker C, Leehey JR, O'Shea CP, "Active vehicle suspension," 2005.

[33] S. J. Anderson ZM, Giovanardi M, Tucker C, Leehey JR, O'Shea CP, "Active vehicle suspension," *Google Patents*, 2017.

[34] M. Peng, X. Guo, J. Zou, and C. Zhang, "Simulation Study on Vehicle Road Performance with Hydraulic Electromagnetic Energy-Regenerative Shock Absorber," *SAE Tech. Pap.*, vol. 2016-April, no. April, 2016, doi: 10.4271/2016-01-1550.

[35] C. Li and P. W. Tse, "Fabrication and testing of an energy-harvesting hydraulic damper," *Smart Mater. Struct.*, vol. 22, no. 6, 2013, doi: 10.1088/0964-1726/22/6/065024.

[36] S. Guo, L. Xu, Y. Liu, X. Guo, and L. Zuo, "Modeling and Experiments of a Hydraulic Electromagnetic Energy-Harvesting Shock Absorber," *IEEE/ASME Trans. Mechatronics*, vol. 22, no. 6, pp. 2684–2694, Dec. 2017, doi: 10.1109/TMECH.2017.2760341.

[37] C. Li, R. Zhu, M. Liang, and S. Yang, "Integration of shock absorption and energy harvesting using a hydraulic rectifier," *J. Sound Vib.*, vol. 333, no. 17, pp. 3904–3916, 2014, doi: 10.1016/j.jsv.2014.04.020.

[38] Y. Zhang, H. Chen, K. Guo, X. Zhang, and S. Eben Li, "Electro-hydraulic damper for energy harvesting suspension: Modeling, prototyping and experimental validation," *Appl. Energy*, vol. 199, pp. 1–12, 2017, doi: 10.1016/j.apenergy.2017.04.085.

[39] Q. Zhou *et al.*, "Global Optimization of the Hydraulic-electromagnetic Energy-harvesting Shock Absorber for Road Vehicles with Human-knowledge-integrated Particle Swarm Optimization Scheme," *IEEE/ASME Trans. Mechatronics*, pp. 1–1, 2021, doi: 10.1109/TMECH.2021.3055815.

[40] L. Bowen, J. Vinolas, J. L. Olazagoitia, and J. Echavarri Otero, "An Innovative Energy Harvesting Shock Absorber System Using Cable Transmission," *IEEE/ASME Trans. Mechatronics*, vol. 24, no. 2, pp. 689–699, 2019, doi: 10.1109/TMECH.2019.2892824.

[41] F. Di Iorio and A. Casavola, "A multiobjective H∞ control strategy for energy harvesting while damping for regenerative vehicle suspension systems," in *2012 American Control Conference (ACC)*, 2012, pp. 491–496, doi: 10.1109/ACC.2012.6314772.

[42] A. Casavola, F. Di Iorio, and F. Tedesco, "A multiobjective H∞ control strategy for energy harvesting in regenerative vehicle suspension systems," *Int. J. Control*, vol. 91, no. 4, pp. 741–754, Apr. 2018, doi: 10.1080/00207179.2017.1293298.

[43] J. T. Scruggs, "Multi-objective nonlinear control of semiactive and regenerative systems," in *Proceedings of the 2010 American Control Conference*, 2010, pp. 726–731, doi: 10.1109/ACC.2010.5530906.

[44] T. H. C. Childs and I. K. Parker, "Power transmission by flat, V and timing belts," 1989, pp. 133–142.

[45] L. Bowen, "Estudio teórico-experimental de sistemas de recuperación de energía en la suspensión de un vehículo automóvil.," Universidad Nebrija, 2018.

[46] T.-T. Tran and H. Hasegawa, "Advanced Passive Suspension with Inerter Devices and Optimization Design for Vehicle Oscillation," *Int. J. Mech. Eng. Robot. Res.*, 2015, doi: 10.18178/ijmerr.4.4.354-360.

[47] L. Marian and A. Giaralis, "Optimal design of a novel tuned mass-damper-inerter (TMDI) passive vibration control configuration for stochastically support-excited structural systems," *Probabilistic Eng. Mech.*, vol. 38, pp. 156–164, 2014, doi: 10.1016/j.probengmech.2014.03.007.

[48] G. H. Z. Liu and M. Z. Q. Chen, "Performance benefits in passive vessel suspensions employing inerters," *Chinese Control Conf. CCC*, vol. 2016-Augus, pp. 8968–8973, 2016, doi: 10.1109/ChiCC.2016.7554789.

[49] and Y. Q. Z. Li, L. Zuo, G. Luhrs, L. Lin, "Electromagnetic Energy-Harvesting Shock Absorbers: Design," *IEEE Trans. Veh. Technol.*, 2013.

[50] M. Izquierdo, "Wheel track variation mechanism comprising inertial dampers to enhance the dynamic performance of an electric three wheeler," Mondragon Unibertsitatea, Mondragon, 2018.

[51] S.-S. Kim and Y. Okada, "Variable Resistance Type Energy Regenerative Damper Using Pulse Width Modulated Step-up Chopper," *J. Vib. Acoust.*, vol. 124, no. 1, pp. 110–115, Jan. 2002, doi: 10.1115/1.1419204.

Alejandro González. Received his Industrial Engineering and PhD degrees from the University of Nebrija in Madrid - Spain. He is currently a researcher in the GREEN group of the Industrial Engineering and Automotive department of the Nebrija University. His research interests are focused on modeling, prototype development and experimental characterization of automotive suspension systems as well as the development of innovative energy recovery systems in vehicle shock absorbers.

José Luis Olazagoitia. Received his Industrial Engineering (Mechanics Intensification) and the PhD degrees from the University of Navarra in San Sebastian - Spain. At present Head of the Vehicle Engineering (GREEN) group, and lecturer at the School of Engineering at Universidad Antonio de Nebrija in Madrid, Spain. Previously, Head of Computer Mechanics at the Automotive Research Centre (CITEAN). Previously technical and R&D manager at PKMtricept SL and product engineer at DANA Automotive. His scientific interests include system optimization, computer simulation, industrial robotics, the study of noise and vibration in brake and suspension systems, tire models, as well as the recovery of residual thermal and mechanical energy and the development of electronic systems and low-cost sensors.

Jordi Viñolas. Received his Industrial Engineering and PhD degrees from the University of Navarra in San Sebastian - Spain. At present Dean and professor at the School of Engineering and Architecture at Universidad Antonio de Nebrija. Previously Head of European Projects at Bantec, a consulting pioneer in the integrated R&D management, for companies, scientific-technological agents, and government. His scientific interests have focused on the fields of machine dynamics, noise and vibration, railway dynamics and road infrastructure. He has published around 50 indexed (JCR) scientific papers and 40 communications in International/National Conferences.

Ibai Ulacia. Received his Bachelor's Degree in Mechanical Engineering, Master's Degree in Industrial Engineering and PhD degrees from Mondragon Unibertsitatea in Mondragon, Spain. He is an accredited Professor in the Department of Mechanical and Industrial Production from Mondragon Unibertsitatea since 2009. Previously, he was a visiting research scholar at the University of Waterloo - Canada. He is currently the Head of the Structural Mechanics and Design (DME) research group. His research interests are oriented to advanced modelling and experimental characterization of machine elements and mechanisms.

Mikel Izquierdo. Received his Bachelor's Degree in Mechanical Engineering, Master's Degree in Industrial Engineering and PhD on the automotive suspension field from Mondragon Unibertsitatea in Mondragon - Spain. He is a lecturer in the Mechanical and Industrial Production Department from Mondragon Unibertsitatea since 2018. He is currently a researcher of the Structural Mechanics and Design (DME) research group. His research interests are oriented to modelling, prototype development and experimental characterization of automotive suspension systems, machine elements and mechanisms.